SCIENCE CHINA
Information Sciences

• **Supplementary File** •

Continuous variable quantum teleportation and remote state preparation between two space-separated local networks

Siyu Ren[1,2†], Dongmei Han[1,2†], Meihong Wang[1,2] & Xiaolong Su[1,2*]

[1]*State Key Laboratory of Quantum Optics and Quantum Optics Devices, Institute of Opto-Electronics, Shanxi University, Taiyuan* 030006*, China;*
[2]*Collaborative Innovation Center of Extreme Optics, Shanxi University, Taiyuan* 030006*, China*

Appendix A Entanglement swapping between two local networks

Appendix A.1 Case-I

The schematic of entanglement swapping between two space-separated local networks A and B is shown in Fig. A1. In the *Case-I*, as shown in Fig. A1(a), two Einstein-Podolsky-Rosen (EPR) states are prepared at the server and distributed in the networks A and B respectively. The modes of the EPR state in the network A are given by

$$\hat{A}_1 = \sqrt{\frac{1}{2}}(\hat{a}_1 + i\hat{a}_2), \tag{A1}$$

$$\hat{A}_2 = \sqrt{\frac{1}{2}}(\hat{a}_1 - i\hat{a}_2), \tag{A2}$$

which is generated by coupling two phase-squeezed states $\hat{a}_1 = \frac{1}{2}(e^r\hat{x}^0 + ie^{-r}\hat{p}^0)$ and $\hat{a}_2 = \frac{1}{2}(e^r\hat{x}^0 + ie^{-r}\hat{p}^0)$ on an balanced optical beam splitter with the relative phase of $\pi/2$ at the server, where $\hat{x}^0$ and $\hat{p}^0$ represent the quadratures of a vacuum state. The modes of the EPR state in the network B are given by

$$\hat{B}_1 = \sqrt{\frac{1}{2}}(\hat{b}_1 + \hat{b}_2), \tag{A3}$$

$$\hat{B}_2 = \sqrt{\frac{1}{2}}(\hat{b}_1 - \hat{b}_2), \tag{A4}$$

which is generated by coupling a phase-squeezed state $\hat{b}_1 = \frac{1}{2}(e^r\hat{x}^0 + ie^{-r}\hat{p}^0)$ and an amplitude-squeezed state $\hat{b}_2 = \frac{1}{2}(e^{-r}\hat{x}^0 + ie^r\hat{p}^0)$ on a balanced optical beam splitter with the relative phase of zero at the server.

To establish the local networks A and B, modes $\hat{A}_2$ and $\hat{B}_2$ are distributed which are expressed by $\hat{A}_2^{'}(\hat{B}_2^{'}) = \sqrt{T}\hat{A}_2(\hat{B}_2) + \sqrt{1-T}(\hat{\nu} + \zeta)$, where $T = 10^{-0.2L/10}$ represents the transmission efficiency in the fiber channel with distance of L between the user and server in a local network, $\hat{\nu}$ represents the vacuum mode with the variance of 1 and ζ is the excess noise with the variance of $\delta = 0.01$ in the calculation. In order to implement entanglement swapping, the mode $\hat{A}_1$ is transmitted to the quantum node B_1 in the network B over fiber channel with $\hat{A}_1^{'} = \sqrt{\eta}\hat{A}_1 + \sqrt{1-\eta}(\hat{\nu} + \zeta)$, where η is the transmission efficiency between two local networks. Joint measurement is performed by coupling modes $\hat{A}_1^{'}$ and $\hat{B}_1$ on a 50:50 beam splitter and measuring the output modes with homodyne detectors, we have $\hat{D} = \sqrt{\frac{1}{2}}(\hat{A}_1^{'} - \hat{B}_1)$ and $\hat{E} = \sqrt{\frac{1}{2}}(\hat{A}_1^{'} + \hat{B}_1)$. Then, the measurement results are fed forward to the mode $\hat{B}_2^{'}$ through classical channels with gain G. Thus, the output beam is

$$\hat{B}_2^{''} = \hat{B}_2^{'} + \sqrt{2}G\hat{x}_D + i\sqrt{2}G\hat{p}_E, \tag{A5}$$

where $\hat{x}_D$ and $\hat{p}_E$ are the amplitude and phase quadratures of the modes $\hat{D}$ and $\hat{E}$, respectively.

After the entanglement swapping, a new entangled state with modes $\hat{C}_1$ and $\hat{C}_2$ is established and the corresponding covariance matrix is given by

$$\sigma_I = \begin{bmatrix} \Delta^2\hat{x}_{C_1} & 0 & C(\hat{x}_{C_1}, \hat{x}_{C_2}) & 0 \\ 0 & \Delta^2\hat{p}_{C_1} & 0 & C(\hat{p}_{C_1}, \hat{p}_{C_2}) \\ C(\hat{x}_{C_2}, \hat{x}_{C_1}) & 0 & \Delta^2\hat{x}_{C_2} & 0 \\ 0 & C(\hat{p}_{C_2}, \hat{p}_{C_1}) & 0 & \Delta^2\hat{p}_{C_2} \end{bmatrix}. \tag{A6}$$

The elements of the above covariance matrix are given by

$$\Delta^2\hat{x}_{C_1} = T(\cosh 2r) - (\delta + 1)(T - 1), \tag{A7}$$

* Corresponding author (email: suxl@sxu.edu.cn)
† Siyu Ren and Dongmei Han have the same contribution to this work.

$$\Delta^2\hat{p}_{C_1} = T(\cosh 2r) - (\delta+1)(T-1), \tag{A8}$$

$$\Delta^2\hat{x}_{C_2} = (1+\delta)(1-\eta)G^2 + (\cosh 2r)((\eta+1)G^2+T) - 2G\sqrt{T}(\sinh 2r) - (\delta+1)(T-1), \tag{A9}$$

$$\Delta^2\hat{p}_{C_2} = (1+\delta)(1-\eta)G^2 + (\cosh 2r)((\eta+1)G^2+T) - 2G\sqrt{T}(\sinh 2r) - (\delta+1)(T-1), \tag{A10}$$

$$C(\hat{x}_{C_1},\hat{x}_{C_2}) = C(\hat{x}_{C_2},\hat{x}_{C_1}) = G\sqrt{\eta}\sqrt{T}\sinh 2r, \tag{A11}$$

$$C(\hat{p}_{C_1},\hat{p}_{C_2}) = C(\hat{p}_{C_2},\hat{p}_{C_1}) = -G\sqrt{\eta}\sqrt{T}\sinh 2r. \tag{A12}$$

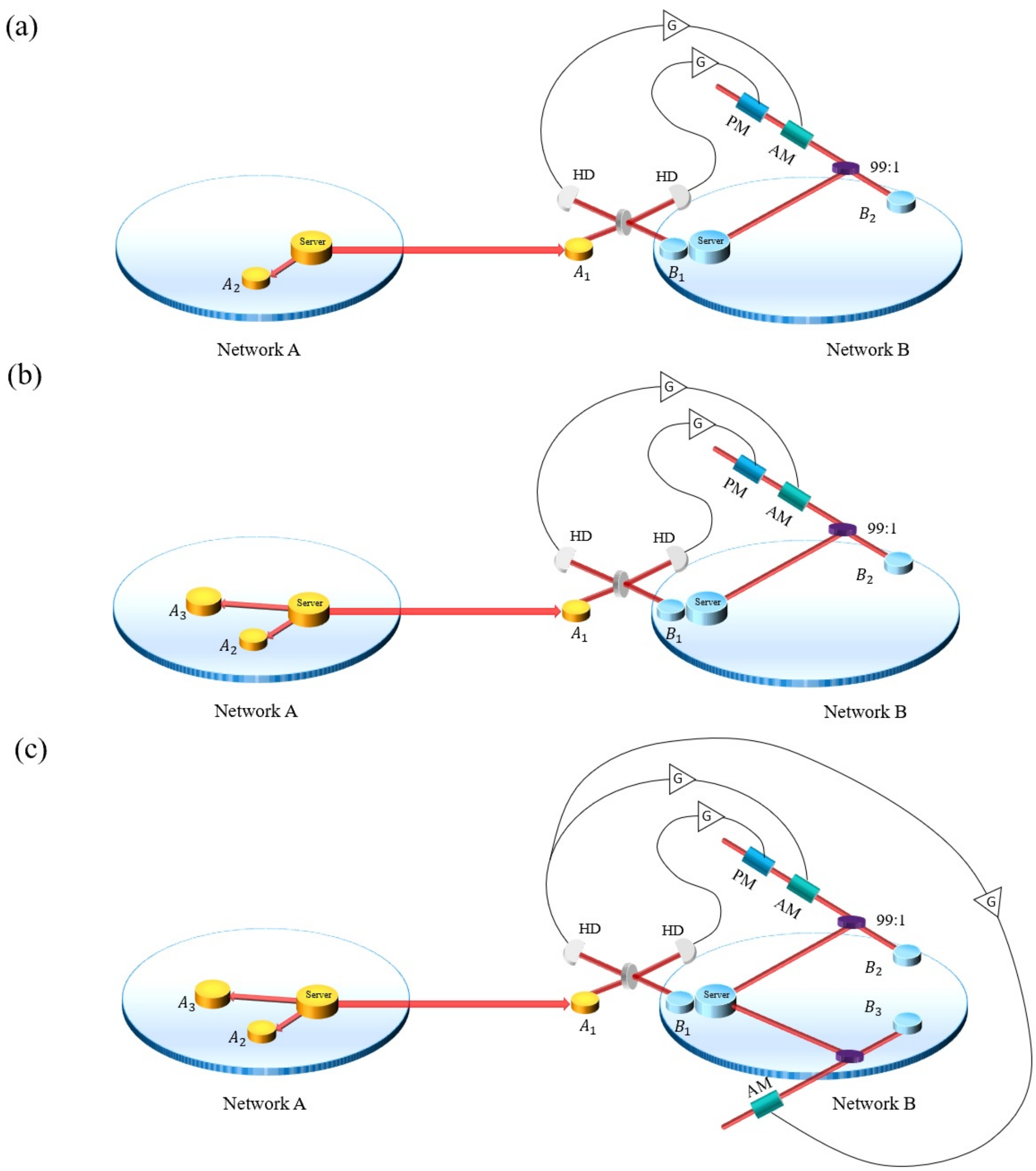

Figure A1 The schematic of entanglement swapping between two space-separated local networks. (a-c) entanglement swapping of the *Case-I*, *Case-II*, and *Case-III*, respectively. AM: amplitude modulator, PM: phase modulator, HD: homodyne detector.

Appendix A.2 Case-II

In the *Case-II*, as shown in Fig. A1(b), a tripartite entangled state and an EPR state are prepared at the server and distributed in the networks A and B respectively. The modes of the tripartite entangled state in the network A are given by

$$\hat{A}_1 = \sqrt{\frac{2}{3}}\hat{a}_1 + \sqrt{\frac{1}{3}}\hat{a}_2, \tag{A13}$$

$$\hat{A}_2 = -\sqrt{\frac{1}{6}}\hat{a}_1 + \sqrt{\frac{1}{3}}\hat{a}_2 + \sqrt{\frac{1}{2}}\hat{a}_3, \tag{A14}$$

$$\hat{A}_3 = -\sqrt{\frac{1}{6}}\hat{a}_1 + \sqrt{\frac{1}{3}}\hat{a}_2 - \sqrt{\frac{1}{2}}\hat{a}_3, \tag{A15}$$

respectively, and the modes $\hat{B}_1$ and $\hat{B}_2$ of the EPR state in the network B are given by

$$\hat{B}_1 = \sqrt{\frac{1}{2}}(\hat{b}_1 + \hat{b}_2), \tag{A16}$$

$$\hat{B}_2 = \sqrt{\frac{1}{2}}(\hat{b}_1 - \hat{b}_2), \tag{A17}$$

where $\hat{a}_2$ and $\hat{b}_1$ are phase-squeezed states, $\hat{a}_1$, $\hat{a}_3$ and $\hat{b}_2$ are amplitud-squeezed states.

To establish the local networks A and B, modes $\hat{A}_2$, $\hat{A}_3$ and $\hat{B}_2$ are distributed which are expressed by $\hat{A}_3^{'} = \sqrt{T}\hat{A}_3 + \sqrt{1-T}(\hat{v}+\zeta)$ and $\hat{A}_2^{'}(\hat{B}_2^{'}) = \sqrt{T}\hat{A}_2(\hat{B}_2) + \sqrt{1-T}(\hat{\nu}+\zeta)$. The process of entanglement swapping is the same to that of the *Case-I*. The covariance matrix of the merged tripartite GHZ states with modes $\hat{C}_1$, $\hat{C}_2$ and $\hat{C}_3$ is given by

$$\sigma_{II} = \begin{bmatrix} \sigma_{C_1} & \sigma_{C_1C_2} & \sigma_{C_1C_3} \\ \sigma_{C_1C_2}^T & \sigma_{C_2} & \sigma_{C_2C_3} \\ \sigma_{C_1C_3}^T & \sigma_{C_3C_4}^T & \sigma_{C_3} \end{bmatrix}, \tag{A18}$$

where

$$\sigma_{C_i} = \begin{bmatrix} \Delta^2\hat{x}_{C_i} & 0 \\ 0 & \Delta^2\hat{p}_{C_i} \end{bmatrix}, \tag{A19}$$

$$\sigma_{C_iC_j} = \begin{bmatrix} C(\hat{x}_{C_i}, \hat{x}_{C_j}) & 0 \\ 0 & C(\hat{p}_{C_i}, \hat{p}_{C_j}) \end{bmatrix}, \tag{A20}$$

and $i, j = 1, 2, 3$. Specifically, the elements of the covariance matrix of the merged tripartite entangled state are given by

$$\Delta^2\hat{x}_{C_1} = (1+\delta)(1-\eta)G^2 + (cosh2r)((\eta+1)G^2 + T) - \frac{1}{3}G(sinh2r)(\eta G + 6\sqrt{T}) + (1+\delta)(1-T), \tag{A21}$$

$$\Delta^2\hat{p}_{C_1} = (1+\delta)(1-\eta)G^2 + (cosh2r)((\eta+1)G^2 + T) - \frac{1}{3}G(sinh2r)(\eta G + 6\sqrt{T}) + (1+\delta)(1-T), \tag{A22}$$

$$\Delta^2\hat{x}_{C_2} = -\frac{1}{3}T(sinh2r) + T(cosh2r) - ((\delta+1)(T-1)), \tag{A23}$$

$$\Delta^2\hat{p}_{C_2} = \frac{1}{3}T(sinh2r) + T(cosh2r) - ((\delta+1)(T-1)), \tag{A24}$$

$$\Delta^2\hat{x}_{C_3} = -\frac{1}{3}T(sinh2r) + T(cosh2r) - ((\delta+1)(T-1)), \tag{A25}$$

$$\Delta^2\hat{p}_{C_3} = \frac{1}{3}T(sinh2r) + T(cosh2r) - ((\delta+1)(T-1)), \tag{A26}$$

$$C(\hat{x}_{C_1}, \hat{x}_{C_2}) = \frac{2}{3}\sqrt{\eta}G\sqrt{T}(sinh2r), \tag{A27}$$

$$C(\hat{x}_{C_1}, \hat{x}_{C_3}) = \frac{2}{3}\sqrt{\eta}G\sqrt{T}(sinh2r), \tag{A28}$$

$$C(\hat{x}_{C_2}, \hat{x}_{C_3}) = \frac{2}{3}T(sinh2r), \tag{A29}$$

$$C(\hat{p}_{C_1}, \hat{p}_{C_2}) = -\frac{2}{3}\sqrt{\eta}G\sqrt{T}(sinh2r), \tag{A30}$$

$$C(\hat{p}_{C_1}, \hat{p}_{C_3}) = -\frac{2}{3}\sqrt{\eta}G\sqrt{T}(sinh2r), \tag{A31}$$

$$C(\hat{p}_{C_2}, \hat{p}_{C_3}) = -\frac{2}{3}T(sinh2r). \tag{A32}$$

Appendix A.3 Case-III

In the *Case-III*, as shown in Fig. A1(c), two tripartite entangled states are prepared at the server and distributed in the networks A and B respectively. The modes of the tripartite entangled state in the network A are given by

$$\hat{A}_1 = \sqrt{\frac{2}{3}}\hat{a}_1 + \sqrt{\frac{1}{3}}\hat{a}_2, \tag{A33}$$

$$\hat{A}_2 = -\sqrt{\frac{1}{6}}\hat{a}_1 + \sqrt{\frac{1}{3}}\hat{a}_2 + \sqrt{\frac{1}{2}}\hat{a}_3, \tag{A34}$$

$$\hat{A}_3 = -\sqrt{\frac{1}{6}}\hat{a}_1 + \sqrt{\frac{1}{3}}\hat{a}_2 - \sqrt{\frac{1}{2}}\hat{a}_3, \tag{A35}$$

respectively, and the modes of the tripartite entangled state in the network B are given by

$$\hat{B}_1 = i\sqrt{\frac{2}{3}}\hat{b}_1 + \sqrt{\frac{1}{3}}\hat{b}_2, \tag{A36}$$

$$\hat{B}_2 = -i\sqrt{\frac{1}{6}}\hat{b}_1 + \sqrt{\frac{1}{3}}\hat{b}_2 + \sqrt{\frac{1}{2}}\hat{b}_3, \tag{A37}$$

$$\hat{B}_3 = -i\sqrt{\frac{1}{6}}\hat{b}_1 + \sqrt{\frac{1}{3}}\hat{b}_2 - \sqrt{\frac{1}{2}}\hat{b}_3, \tag{A38}$$

where $\hat{a}_2$, $\hat{b}_1$ and $\hat{b}_2$ are phase-squeezed states, $\hat{a}_1$, $\hat{a}_3$ and $\hat{b}_3$ are amplitude-squeezed states.

To establish the local networks A and B, modes $\hat{A}_2$, $\hat{A}_3$, $\hat{B}_2$ and $\hat{B}_3$ are distributed which are expressed by $\hat{A}_2^{'} = \sqrt{T}\hat{A}_2 + \sqrt{1-T}(\hat{\nu}+\zeta)$ and $\hat{A}_3^{'}(\hat{B}_3^{'}) = \sqrt{T}\hat{A}_3(\hat{B}_3) + \sqrt{1-T}(\hat{\upsilon}+\zeta)$. The measurement results of joint measurement on modes $\hat{A}_1$ and $\hat{B}_1$ are fed forward to the modes $\hat{B}_2^{'}$ and $\hat{B}_3^{'}$ through classical channels. The output modes are expressed as

$$\hat{B}_2^{''} = \hat{B}_2^{'} + \sqrt{2}G\hat{x}_D + i\sqrt{2}G\hat{p}_E, \tag{A39}$$

$$\hat{B}_3^{''} = \hat{B}_3^{'} + \sqrt{2}G\hat{x}_D. \tag{A40}$$

After the entanglement swapping, a four-partite entangled state with modes $\hat{C}_1$, $\hat{C}_2$, $\hat{C}_3$ and $\hat{C}_4$ is established, whose covariance matrix is given by

$$\sigma_{III} = \begin{bmatrix} \sigma_{C_1} & \sigma_{C_1C_2} & \sigma_{C_1C_3} & \sigma_{C_1C_4} \\ \sigma_{C_1C_2}^T & \sigma_{C_2} & \sigma_{C_2C_3} & \sigma_{C_2C_4} \\ \sigma_{C_1C_3}^T & \sigma_{C_3C_4}^T & \sigma_{C_3} & \sigma_{C_3C_4} \\ \sigma_{C_1C_4}^T & \sigma_{C_2C_4}^T & \sigma_{C_3C_4}^T & \sigma_{C_4} \end{bmatrix}, \tag{A41}$$

where

$$\sigma_{C_i} = \begin{bmatrix} \Delta^2\hat{x}_{C_i} & 0 \\ 0 & \Delta^2\hat{p}_{C_i} \end{bmatrix}, \tag{A42}$$

$$\sigma_{C_iC_j} = \begin{bmatrix} C(\hat{x}_{C_i}, \hat{x}_{C_j}) & 0 \\ 0 & C(\hat{p}_{C_i}, \hat{p}_{C_j}) \end{bmatrix}, \tag{A43}$$

and $i, j = 1, 2, 3, 4$. Specifically, the elements of the covariance matrix of the output state are given by

$$\Delta^2\hat{x}_{C_1} = -\frac{1}{3}T(sinh2r) + T(cosh2r) - ((\delta+1)(T-1)), \tag{A44}$$

$$\Delta^2\hat{p}_{C_1} = \frac{1}{3}T(sinh2r) + T(cosh2r) - ((\delta+1)(T-1)), \tag{A45}$$

$$\Delta^2\hat{x}_{C_2} = -\frac{1}{3}T(sinh2r) + T(cosh2r) - ((\delta+1)(T-1)), \tag{A46}$$

$$\Delta^2\hat{p}_{C_2} = \frac{1}{3}T(sinh2r) + T(cosh2r) - ((\delta+1)(T-1)), \tag{A47}$$

$$\Delta^2\hat{x}_{C_3} = \frac{1}{3}e^{-2r}(-3e^{2r}(\delta(\eta-1)G^2 + (\eta-1)G^2 + \delta(T-1) + T - 1) + e^{4r}((\eta+1)G^2 - 2G\sqrt{T} + T) + 2((\eta+1)G^2 + G\sqrt{T} + T)), \tag{A48}$$

$$\Delta^2\hat{p}_{C_3} = \frac{1}{3}e^{-2r}(\eta G^2 - 3e^{2r}(\delta(\eta-1)G^2 + (\eta-1)G^2 + \delta(T-1) + T - 1) + 2e^{4r}((\eta+1)G^2 - G\sqrt{T} + T) + G^2 + 2G\sqrt{T} + T), \tag{A49}$$

$$\Delta^2\hat{x}_{C4} = \frac{1}{3}e^{-2r}(-3e^{2r}(\delta(\eta-1)G^2 + (\eta-1)G^2 + \delta(T-1) + T - 1) + e^{4r}((\eta+1)G^2 - 2G\sqrt{T} + T) + 2((\eta+1)G^2 + G\sqrt{T} + T)), \tag{A50}$$

$$\Delta^2\hat{p}_{C_4} = \frac{1}{3}T(sinh2r) + T(cosh2r) - ((\delta+1)(T-1)), \tag{A51}$$

$$C(\hat{x}_{C_1}, \hat{x}_{C_2}) = \frac{2}{3}T(sinh2r), \tag{A52}$$

$$C(\hat{x}_{C_1}, \hat{x}_{C_3}) = C(\hat{x}_{C_1}, \hat{x}_{C_4}) = \frac{2}{3}\sqrt{\eta}G\sqrt{T}(sinh2r), \tag{A53}$$

$$C(\hat{x}_{C_2},\hat{x}_{C_3}) = C(\hat{x}_{C_2},\hat{x}_{C_4}) = \frac{2}{3}\sqrt{\eta}G\sqrt{T}(sinh2r), \tag{A54}$$

$$C(\hat{x}_{C_3},\hat{x}_{C_4}) = \frac{1}{3}e^{-2r}(2\eta G^2 - 3(\delta+1)(\eta-1)G^2e^{2r} + e^{4r}((\eta+1)G^2 - 2G\sqrt{T} + T) + 2G^2 + 2G\sqrt{T} - T), \tag{A55}$$

$$C(\hat{p}_{C_1},\hat{p}_{C_2}) = -\frac{2}{3}\sqrt{\eta}G\sqrt{T}(sinh2r), \tag{A56}$$

$$C(\hat{p}_{C_1},\hat{p}_{C_3}) = -\frac{2}{3}\sqrt{\eta}G\sqrt{T}(sinh2r), \tag{A57}$$

$$C(\hat{p}_{C_1},\hat{p}_{C_4}) = C(\hat{p}_{C_2},\hat{p}_{C_4}) = 0, \tag{A58}$$

$$C(\hat{p}_{C_2},\hat{p}_{C_3}) = -\frac{2}{3}\sqrt{\eta}G\sqrt{T}(sinh2r), \tag{A59}$$

$$C(\hat{p}_{C_3},\hat{p}_{C_4}) = -\frac{2}{3}\sqrt{T}(G+\sqrt{T})(sinh2r). \tag{A60}$$

We choose the optimal gain G to maximize the entanglement of the new merged entangled state. The optimal gain G at different transmission efficiency η is shown in the Table A1 where we choose $r = 1.15$, $\delta = 0.01$, and L=5 km.

Table A1 The optimum gains in entanglement swapping at different transmission distances

Distance	0 km	5 km	10 km	20 km	30 km	40 km	50 km	60 km	70 km	80 km
G(*case-I*)	0.874	0.854	0.836	0.804	0.780	0.763	0.751	0.743	0.737	0.734
G(*case-II*)	0.89	0.88	0.88	0.86	0.84	0.82	0.81	0.79	0.78	0.78
G(*case-III*)	0.87	0.83	0.81	0.78	0.775	0.77	0.77	0.765	0.76	0.76

Appendix A.4 Entanglement swapping between two local networks with n and m modes

As shown in Fig. 1, there are two continuous variable (CV) Greenberger-Horne-Zeilinger (GHZ) states with n modes ($\hat{A}_1$, $\hat{A}_2$, . . . , $\hat{A}_n$) in the network A and m modes ($\hat{B}_1$, $\hat{B}_2$, . . . , $\hat{B}_m$) in the network B respectively. In case of infinite squeezing ($r \to \infty$), the CV GHZ states are the eigenstate with total momentum (phase quadrature) zero and relative positions (amplitude quadrature) zero, which are expressed by

$$\hat{x}_{A_i} - \hat{x}_{A_j} = 0,\ (i,\ j = 1,\ 2,\ 3,\ .\ .\ .\ ,\ n), \tag{A61}$$

$$\hat{p}_{A_1} + \hat{p}_{A_2} + \hat{p}_{A_3} + .\ .\ . + \hat{p}_{A_n} = 0, \tag{A62}$$

$$\hat{x}_{B_k} - \hat{x}_{B_l} = 0,\ (k,\ l = 1,\ 2,\ 3,\ .\ .\ .\ ,\ m), \tag{A63}$$

$$\hat{p}_{B_1} + \hat{p}_{B_2} + \hat{p}_{B_3} + .\ .\ . + \hat{p}_{B_m} = 0. \tag{A64}$$

In the entanglement swapping, modes $\hat{A}_1$ and $\hat{B}_1$ are coupled on a 50:50 beam splitter firstly. Then, two output modes of the beam splitter which are proportional to $\frac{1}{\sqrt{2}}(\hat{x}_{A_1} - \hat{x}_{B_1})$ and $\frac{1}{\sqrt{2}}(\hat{p}_{A_1} + \hat{p}_{B_1})$ are measured by two homodyne detectors. Finally, the measurement result of $\frac{1}{\sqrt{2}}(\hat{x}_{A_1} - \hat{x}_{B_1})$ is fed forward to the rest modes $\hat{B}_2$, $\hat{B}_3$, . . . , $\hat{B}_m$ in the network B and $\frac{1}{\sqrt{2}}(\hat{p}_{A_1} + \hat{p}_{B_1})$ is fed forward to arbitrary one mode in the network B, for example $\hat{B}_2$. After entanglement swapping, the new merged entangled state with n+m-2 modes ($\hat{C}_1$, $\hat{C}_2$, . . . , $\hat{C}_{n+m-2}$) is established, in which the modes $\hat{C}_1$, $\hat{C}_2$, . . . , $\hat{C}_{n-1}$ corresponding to the remaining modes of $\hat{A}_2$, $\hat{A}_3$, . . . , $\hat{A}_n$ in the network A, whose quadratures are given by

$$\hat{x}_{C_1} = \hat{x}_{A_2},\ \hat{x}_{C_2} = \hat{x}_{A_3},\ .\ .\ .\ , \hat{x}_{C_{n-1}} = \hat{x}_{A_n}, \tag{A65}$$

$$\hat{p}_{C_1} = \hat{p}_{A_2},\ \hat{p}_{C_2} = \hat{p}_{A_3},\ .\ .\ .\ , \hat{p}_{C_{n-1}} = \hat{p}_{A_n}, \tag{A66}$$

and the modes $\hat{C}_n$, $\hat{C}_{n+1}$, . . . , $\hat{C}_{n+m-2}$ corresponding to the remaining modes of $\hat{B}_2$, $\hat{B}_3$, . . . , $\hat{B}_m$ in the network B, whose quadratures are given by

$$\begin{aligned} \hat{x}_{C_n} &= \hat{x}_{B_2} + G(\hat{x}_{A_1} - \hat{x}_{B_1}) \\ \hat{x}_{C_{n+1}} &= \hat{x}_{B_3} + G(\hat{x}_{A_1} - \hat{x}_{B_1}) \\ &\vdots \\ \hat{x}_{C_{n+m-2}} &= \hat{x}_{B_m} + G(\hat{x}_{A_1} - \hat{x}_{B_1}) \end{aligned} \tag{A67}$$

$$\begin{aligned} \hat{p}_{C_n} &= \hat{p}_{B_2} + G(\hat{p}_{A_1} + \hat{p}_{B_1}) \\ \hat{p}_{C_{n+1}} &= \hat{p}_{B_3} \\ &\vdots \\ \hat{p}_{C_{n+m-2}} &= \hat{p}_{B_m} \end{aligned} \tag{A68}$$

where G represents the classical gain in the entanglement swapping. In case of infinite squeezing ($r \to \infty$), we have the optimal gain $G = 1$.

Based on Eq. (A61) and Eq. (A65), we have the quantum correlations for the amplitude quadratures of modes $\hat{C}_i$ and $\hat{C}_j$ located in the network A, which are expressed by

$$\hat{x}_{C_i} - \hat{x}_{C_j} = (\hat{x}_{A_{i+1}} - \hat{x}_{A_{j+1}}) = 0,\ (i,\ j = 1,\ 2,\ 3,\ .\ .\ .\ ,\ n-1) \tag{A69}$$

Similarly, based on Eq. (A63) and Eq. (A67), we have the quantum correlations for the amplitude quadratures of modes $\hat{C}_k$ and $\hat{C}_l$ located in the network B, which are expressed by

$$\hat{x}_{C_k} - \hat{x}_{C_l} = (\hat{x}_{A_{k+2-n}} - \hat{x}_{A_{l+2-n}}) = 0,\ (k,\ l = n,\ n+1,\ n+2,\ ...,\ n+m-2) \tag{A70}$$

Based on Eqs. (A61), (A63), (A65) and (A67), we can prove that the modes $\hat{C}_p$ in the network A and $\hat{C}_q$ in the network B present the quantum correlations of

$$\hat{x}_{C_p} - \hat{x}_{C_q} = (\hat{x}_{A_{p+1}} - \hat{x}_{A_1}) + (\hat{x}_{B_1} - \hat{x}_{B_{q+2-n}}) = 0,\ (p = 1,\ 2,\ 3,\ ...,\ n,\ q = n,\ n+1,\ n+2,\ ...,\ n+m-2) \tag{A71}$$

Based on Eqs. (A62), (A64), (A66) and (A68), the total momentum of network C can be expressed as

$$\hat{p}_{C_1} + \hat{p}_{C_2} + \hat{p}_{C_3} + \ ...\ + \hat{p}_{C_{n+m-2}} = (\hat{p}_{A_1} + \hat{p}_{A_2} + \hat{p}_{A_3} + \ ...\ + \hat{p}_{A_n}) + (\hat{p}_{B_1} + \hat{p}_{B_2} + \hat{p}_{B_3} + \ ...\ + \hat{p}_{B_m}) = 0 \tag{A72}$$

The new entangled state is a CV GHZ state with n+m-2 modes, which has quantum correlations in amplitude and phase quadratures expressed by

$$\hat{x}_{C_i} - \hat{x}_{C_j} = 0(i,\ j = 1,\ 2,\ 3,\ ...,\ n+m-2) \tag{A73}$$

$$\hat{p}_{C_1} + \hat{p}_{C_2} + \hat{p}_{C_3} + \ ...\ + \hat{p}_{C_{n+m-2}} = 0 \tag{A74}$$

Thus, it is obvious that the (2,3) and (3,3) cases can be extended to the arbitrary (n, m) case.

Appendix B Quantum teleportation between two local networks

Appendix B.1 Quantum teleportation in the *Case-II*

In the *Case-II*, quantum teleportation from $\hat{C}_1$ in the network A to $\hat{C}_2$ in the network B is implemented with the assistance of $\hat{C}_3$. The teleported field is given by

$$\hat{x}_{tel} = \hat{x}_2 + \sqrt{2}g\hat{x}_u, \tag{B1}$$

$$\hat{p}_{tel} = \hat{p}_2 + \sqrt{2}g\hat{p}_v + g_1\hat{p}_3. \tag{B2}$$

Correspondingly, the variances of amplitude and phase quadratures of the teleported field are given by

$$\begin{aligned}\sigma^x = \Delta^2\hat{x}_{tel} =& \frac{1}{6}e^{-2r}(-6e^{2r}(\delta g^2(T-1) + g^2(T-2) + \delta(\eta-1)G^2 + (\eta-1)G^2 + \delta(T-1) + T - 1)\\ &+ e^{4r}((2g^2+3)T - 2G\sqrt{T}(2g\sqrt{\eta}+3) + (2\eta+3)G^2) + 4g^2T + 4\sqrt{\eta}gG\sqrt{T} + 4\eta G^2 + 3G^2 + 6G\sqrt{T} + 3T),\end{aligned} \tag{B3}$$

$$\begin{aligned}\sigma^p = \Delta^2\hat{p}_{tel} =& \frac{1}{3}((\sinh 2r)(g^2T - 2G\sqrt{T}(2g\sqrt{\eta}+3) - 4g_1(gT + \sqrt{\eta}G\sqrt{T}) + g_1^2T + \eta G^2) + 3(\cosh 2r)((g^2+1)T + g_1^2T\\ &+ (\eta+1)G^2) - 3(\delta g^2(T-1) + g^2(T-2) + (\delta+1)g_1^2(T-1) + \delta(\eta-1)G^2 + (\eta-1)G^2 + \delta(T-1) + T - 1)).\end{aligned} \tag{B4}$$

where $g = g_1 = 1$ are gains of classical channels for quantum teleportation.

Appendix B.2 Quantum teleportation in the *Case-III*

In the *Case-III*, quantum teleportation from $\hat{C}_1$ in the network A to $\hat{C}_2$ in the network B is implemented with the assistance of $\hat{C}_3$ and $\hat{C}_4$. The teleported field is given by

$$\hat{x}_{tel} = \hat{x}_2 + \sqrt{2}g\hat{x}_u, \tag{B5}$$

$$\hat{p}_{tel} = \hat{p}_2 + \sqrt{2}g\hat{p}_v + g_1\hat{p}_3 + g_2\hat{p}_4. \tag{B6}$$

Correspondingly, the variance of amplitude and phase quadratures of the teleported fields are given by

$$\begin{aligned}\sigma^x = \Delta^2\hat{x}_{tel} =& \frac{1}{3}e^{-2r}(-3e^{2r}(\delta g^2(T-1) + g^2(T-2) + \delta(\eta-1)G^2 + (\eta-1)G^2 + \delta(T-1) + T - 1)\\ &+ e^{4r}((g^2+1)T - 2G\sqrt{T}(g\sqrt{\eta}+1) + (\eta+1)G^2) + 2((g^2+1)T + G\sqrt{T}(g\sqrt{\eta}+1) + (\eta+1)G^2)),\end{aligned} \tag{B7}$$

$$\begin{aligned}\sigma^p = \Delta^2\hat{p}_{tel} =& \frac{1}{3}e^{-2r}(e^{2r}(-3(T-1)(\delta+\delta g^2) - 4g_1\sqrt{T}(\sinh 2r)(g\sqrt{T} + \sqrt{\eta}G) - 4g_2\sqrt{T}(G+\sqrt{T})\sinh 2r + g_1^2(T(\sinh 2r)\\ &+ 3T(\cosh 2r) - 3(\delta+1)(T-1)) + g_2^2(T(\sinh 2r) + 3T(\cosh 2r) - 3(\delta+1)(T-1)) - 3\delta(\eta-1)G^2) - 3e^{2r}(g^2(T-2)\\ &+ (\eta-1)G^2 + T - 1) + 2e^{4r}((g^2+1)T - G\sqrt{T}(g\sqrt{\eta}+1) + (\eta+1)G^2) + (g^2+1)T + 2G\sqrt{T}(g\sqrt{\eta}+1) + (\eta+1)G^2),\end{aligned} \tag{B8}$$

where $g = g_1 = g_2 = 1$ are gains of classical channels for quantum teleportation.

Appendix C The fidelity of the squeezed thermal state

The fidelity of the remotely prepared squeezed thermal states is obtained by calculating the overlap between the ideal squeezed thermal state and the remotely prepared state. Here, we take the *Case-I* to elaborate on the process of obtaining fidelity. The Wigner function of the remotely prepared state is given by :

$$W(x_{C_2}, p_{C_2}) = \int\int dx_1 dp_1 W_2 \times W[\Pi_x](x_{C_1}), \tag{C1}$$

where W_2 is the Wigner function of the merged EPR entangled state which can be obtained from the covariance matrix of the merged EPR entangled state according to Eq. (6) in the main text.

The Wigner function of the ideal squeezed thermal state is expressed by

$$W(x_{C_k}, p_{C_k}) = \frac{1}{2\pi(1+2\overline{n})} \exp\left\{-(\frac{x_k^2}{e^{-2r}} + \frac{p_k^2}{e^{2r}})/2(1+2\overline{n})\right\}, \tag{C2}$$

where $\overline{n}$ and r are the average photon number and squeezing parameter of the ideal squeezed thermal state, respectively. The fidelity is calculated by

$$F_{RSP} = 2\pi \int\int dxdp W(x_{C_k}, p_{C_k}) W(x_{C_2}, p_{C_2}) \tag{C3}$$

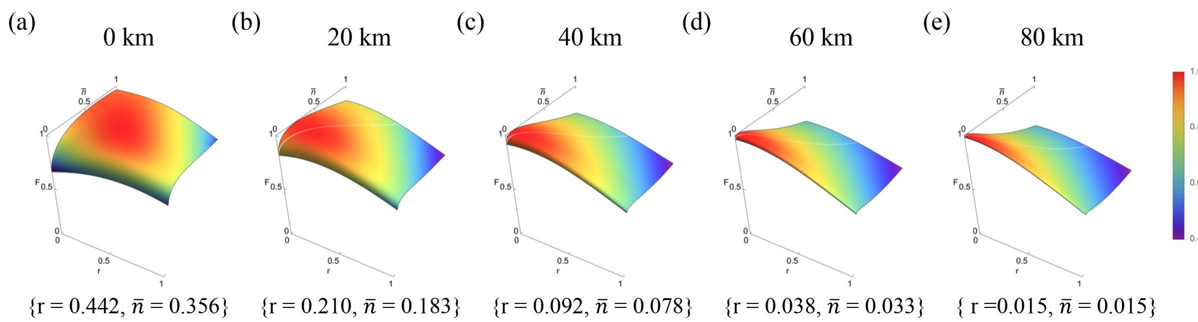

Figure C1 The dependence of the fidelity F_{RSP} on the squeezing parameter r and average photon number $\overline{n}$ of the remotely prepared squeezed thermal state at different distance L_{AB}.

Figure C1 shows the dependence of the fidelity F_{RSP} on the squeezing parameter r and average photon number $\overline{n}$ of the remotely prepared state. The parameter of the squeezing parameter r and average photon number $\overline{n}$ are obtained when the fidelity reaches its maximum. At the maximum fidelity which equals 1, the corresponding squeezing parameter r and average photon number $\overline{n}$ are shown below the three-dimensional plot at the distances of 0 km, 20 km, 40 km, 60 km, and 80 km, respectively. With the increase of the transmission distance, the squeezing parameter r and average photon number $\overline{n}$ decrease, while the fidelity remains unit. The fidelity F_{RSP}, the squeezing parameter r, and average photon number $\overline{n}$ of other remotely prepared states at different distances in other cases can be calculated in the same way. The squeezing level can be obtained from the squeezing parameter by $10\lg(e^{-2r})$.